An Optoelectronic Read-Out IC for Indoor-Monitoring LiDAR Sensors in 180-nm CMOS

Shinhae Choi[1,2], Yeojin Chon[1,2], and Sung Min Park[1,2,a]
[1]Division of Electronic and Semiconductor Engineering, Ewha Womans University, Seoul, 03760, R. O. Korea
[2]Graduate Program in Smart Factory, Ewha Womans University, Seoul, 03760, R. O. Korea
E-mail : rora0414@ewhain.net, wjsdulws7@gmail.com, smpark@ewha.ac.kr

***Abstract* - This paper presents an optoelectronic read-out integrated circuit (ROIC) for the applications of indoor-monitoring LiDAR sensors by utilizing a 180-nm CMOS technology, which consists of a spatially modulated P^+/N-well avalanche photodiode, amplitude-to-voltage (A2V) converter, and time-to-voltage (T2V) converter, respectively. Post-layout simulations reveal that the analog A2V converter can recover the input currents of 5 ~ 500 μApp with an almost linear step with the aid of gain control scheme, while the T2V converter can restore 50 μA_{pp} ~ 1.1 mA_{pp} input currents. The whole 8x8 ROIC array dissipates 262 mW in total from a single 1.8-V supply and occupies an area of 2.1 x 2.0 mm^2 including I/O pads.**

***Keywords*— A2V, T2V, APD, LiDAR, optoelectronic, TIA**

I. INTRODUCTION

Light detection and ranging (LiDAR) sensors have proliferated in several fields including autonomous cars, remote sensing applications to observe forestry, cryosphere, aerosols, and clouds, indoor-monitoring sensors to help either nurses or families take care of senile dementia patients, and etc. It is well known that the state-of-the art LiDAR sensors mostly utilize the pulsed time-of-flight (ToF) mechanism. Hence, light pulse signals are emitted from their laser diode drivers to the surrounding targets located within a feasible range and then the reflected light signals are detected by their sensitive optical receivers. The distance to targets is easily estimated by measuring the time interval between their transmitted (a.k.a. START) pulses and the reflected (a.k.a. STOP) pulses.

In South Korea, it has recently been a serious issue that the population of seniors older than 65 has become more than 20 percent. This phenomenon might "lead to perilous social problems such as an increase in single elders and senile dementia patients. Normally, seniors might suffer from declining cognitive ability and tend to face the dangers of falling accidents, heart attack during sleep, and even suicide [1].

a. Corresponding author; smpark@ewha.ac.kr

Manuscript Received Mar. 5, 2024, Revised May 17, 2024, Accepted May 26, 2024

Moreover, the Korean Ministry of Health and Welfare has predicted that a million population of elders that is almost 10 % of seniors might suffer from dementia in 2025. Additionally, some seniors might suffer from falls, which, however, demand extremely high costs—almost two trillion Korean won. In addition, single elders who have lost their spouses and live alone are easily afraid to experience sudden death from heart attack and many other illnesses owing to aging. Even for other seniors who live with their own families, it is very difficult to cope with the disastrous situations of sudden falls and even death afterwards.

Therefore, it is definitely desirable to install tiny sensitive LiDAR sensors on the ceilings in their homes and to deliver warning messages to either their family or visiting nurses instantly, so that they can recognize the dangerous situations right after any kind of accidents at home. Then, the seniors' invaluable lives can be saved and prolonged together with human dignity. For these purposes, a small low-power LiDAR sensor realized in a low-cost CMOS technology can be a feasible solution because it can precisely provide every necessary information of seniors such as falling accidents. Besides, it can demonstrate numerous advantages over conventional RF sensors, including their robustness against severe RF interference [4,5]. Previously, a number of ROICs have been suggested [6-8], in which off-chip avalanche photodiodes (APDs) were mostly integrated on PC-boards via bond-wires. However, this bond-wire interconnection may lead to considerable increase of packaging cost in the cases of multi-channel receiver arrays, and mandate on-chip electrostatic discharge protection diodes which, however, deteriorate the receiver bandwidth and worsen the noise performance. Fig. 1 shows the block diagram of a typical indoor-monitoring LiDAR sensor, where the laser diode driver (LDD) emits light pulses to a target that is a senior in this figure. Thereafter, the reflected light pulses are detected by the optical receiver array which converts the light pulses into current signals with on-chip APDs and eventually generates digital codes, so that the distance (or depth) information to the target can be estimated. Hence, the abrupt falling accidents can be delivered to either families or nurses in real-time. In this work, a CMOS 8x8 ROIC array is presented for indoor-monitoring LiDAR sensor applications, of which single cell comprises a P^+/N-well APD, a voltage-mode transimpedance amplifier (VCF-TIA), an amplitude-to-voltage (A2V) converter, and a time-to-voltage (T2V) converter.

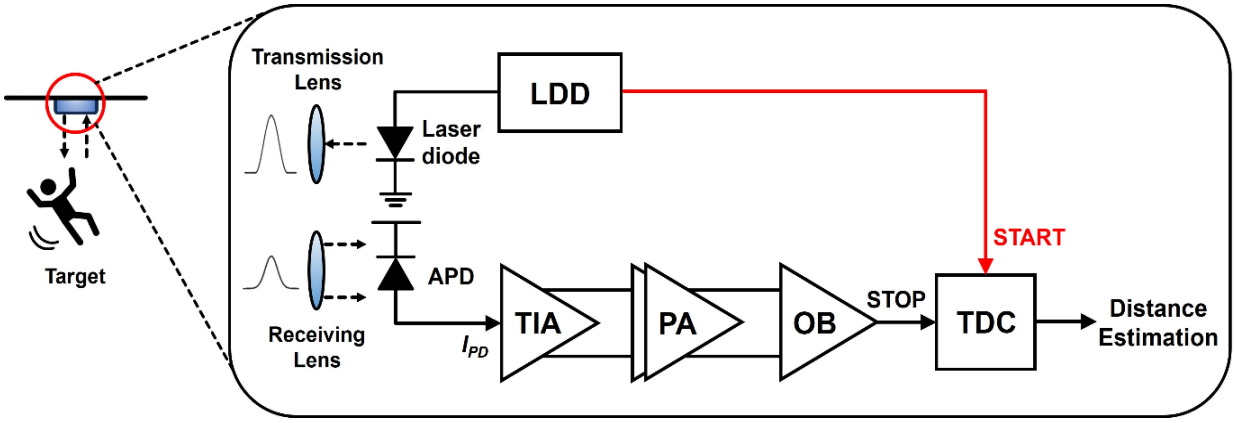

Fig. 1. Block diagram of a typical LiDAR sensor.

Section II describes the structure of the realized CMOS on-chip APD, the architecture of the proposed ROIC circuit, the layout of the 8x8 ROIC, and its simulation results. Then, a conclusion is followed.

II. ARCHITECTURE

A. Circuit Description

Fig. 2 depicts the cross-sectional view and the layout of the P⁺/N-well on-chip APD [9], which utilizes a metal layer to block part of the active area, thus reducing the notoriously slow diffusion currents of the APDs. Then, the bandwidth of the on-chip APDs can be extended further even with the expense of the responsivity [6]. It is well known that CMOS on-chip APDs are very attractive because they can lower the total cost of multi-channel modules under the condition that the on-chip APD should provide substantial optical responsivities. Since the on-chip APDs are implemented in the CMOS technology, the utilized wavelength is 850 nm. Therefore, it might be dangerous in terms of eye-safety when a rather large optical power is emitted from the LDD.

Fig. 3 shows the block diagram of the optoelectronic Rx, which consists of A2V and T2V, and Fig. 4 (a) depicts the VCF-TIA which comprises a conventional voltage-mode inverter (INV) input stage with a feedback resistor (RF), a feedforward common-source amplifier with its gate connected to the gates of the INV stage.

According to the small signal analysis of the simplified feedforward input stage, the transimpedance gain is given by,

$$Z_T(0) = -\frac{(g_{m1}+g_{m2}+g_{m3})R_F-1}{g_{m1}+g_{m2}+g_{m3}+\frac{1}{r_{o1}||r_{o2}||r_{o3}||R_L}} \cong -R_F \qquad (1)$$

The input-referred noise current spectral density is given by,

$$\overline{I^2}_{n,TIA}(f) \cong \frac{4kT}{R_F} + 4kT\Gamma\left(\frac{1}{g_{m1}}+\frac{1}{g_{m2}}\right)\times\left[(2\pi C_T)^2 f^2 + \frac{1}{R_F^2}\right] + 4kT\left(\Gamma\frac{1}{g_{m3}} + R_G\right)\times\left[(2\pi C_T)^2 f^2 + \frac{1}{R_F^2}\right] \cong \frac{4kT}{R_F} + 4kT\Gamma\left(\frac{1}{g_{m1}} + \frac{1}{g_{m2}} + \frac{1}{g_{m3}}\right)\times(2\pi C_T)^2 f^2 \qquad (2)$$

where k is the Boltzmann's constant, T is the absolute temperature, and $\Gamma(\approx 2)$ is the Ogawa's noise factor of a MOSFET.

Furthermore, C_T ($= C_{PD} + C_{in,M1} + C_{in,M2}$) represents the total capacitance at the input node of the VCF-TIA which includes the photodiode capacitance (C_{PD}) and the input capacitance of the INV input stage, i.e., $C_{in,M1} + C_{in,M2} = C_{gs1} + C_{gs2} + (1 + A_v)\cdot(C_{gd1} + C_{gd2})$.

It is noted that R_G is set to 1 kΩ in this work so that the noise contribution from R_G can be negligible.

Then, the input-referred mean-square noise current is given by,

$$\overline{i^2}_{n,TIA} \cong \frac{4kT}{R_F}BW_{n1} + \frac{4kT\Gamma}{3}C_T^2 BW_{n2}^2\left(\frac{1}{g_{m1}}+\frac{1}{g_{m2}}+\frac{1}{g_{m3}}\right) \qquad (3)$$

where BW_{n1} is the noise bandwidth for white noise and BW_{n2} is the noise bandwidth for f^2 noise. For $Q = 1/\sqrt{2}$, $BW_{n1} \approx 1.11\cdot BW^3{}_{3dB}$ and $BW_{n2} \approx 1.49\cdot BW_{3dB}$ [7].

The value of R_L is selected to be a few tens of kilo-ohm. Then, the bias current (I_2) of M_3 can be mostly supplied through the PMOS (M_2) of the INV stage, because the DC drain voltage of M_2 is fixed by the action of the INV stage via the feedback resistor (R_F). Hence, this action enables to boost the transconductance (g_{m2}) of M_2 and helps to reduce the noise current spectral density of the feedforward TIA.

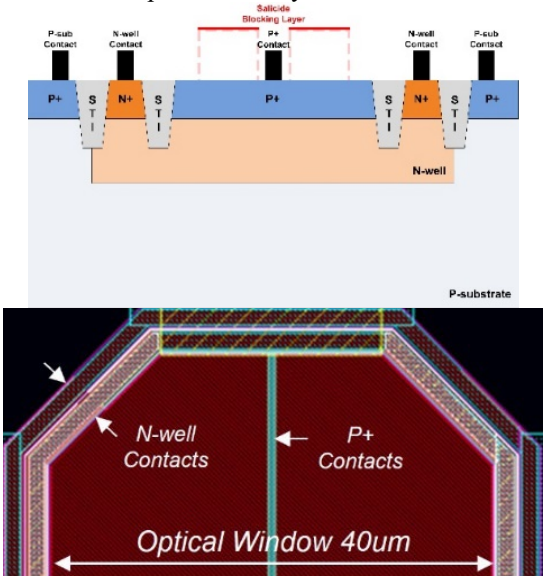

Fig. 2. Cross-section of the P⁺/N-well on-chip APD, and its layout.

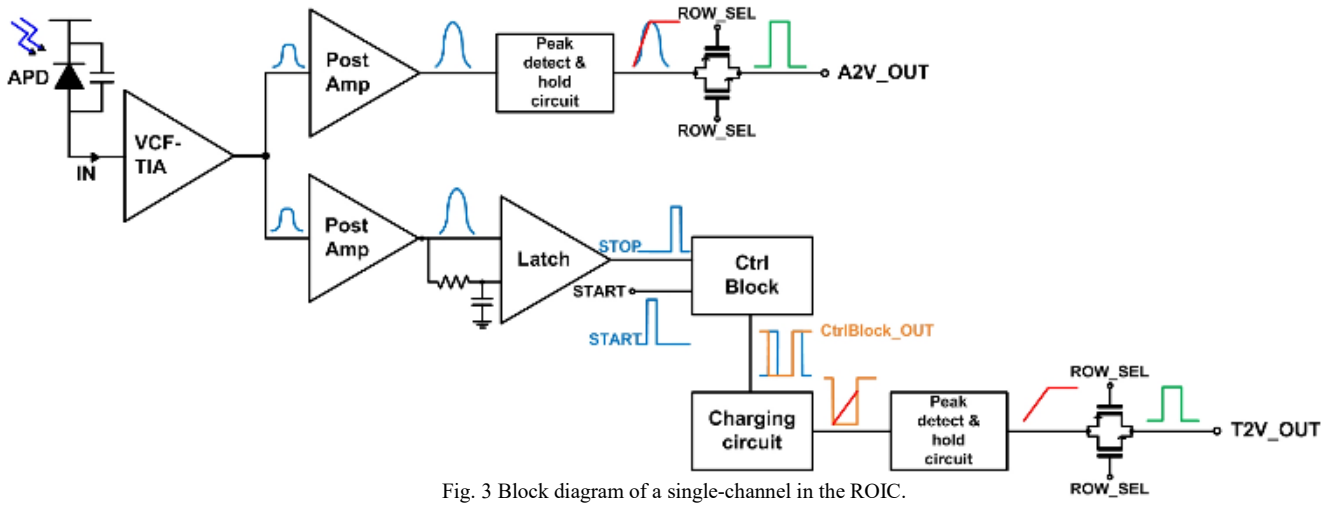

Fig. 3 Block diagram of a single-channel in the ROIC.

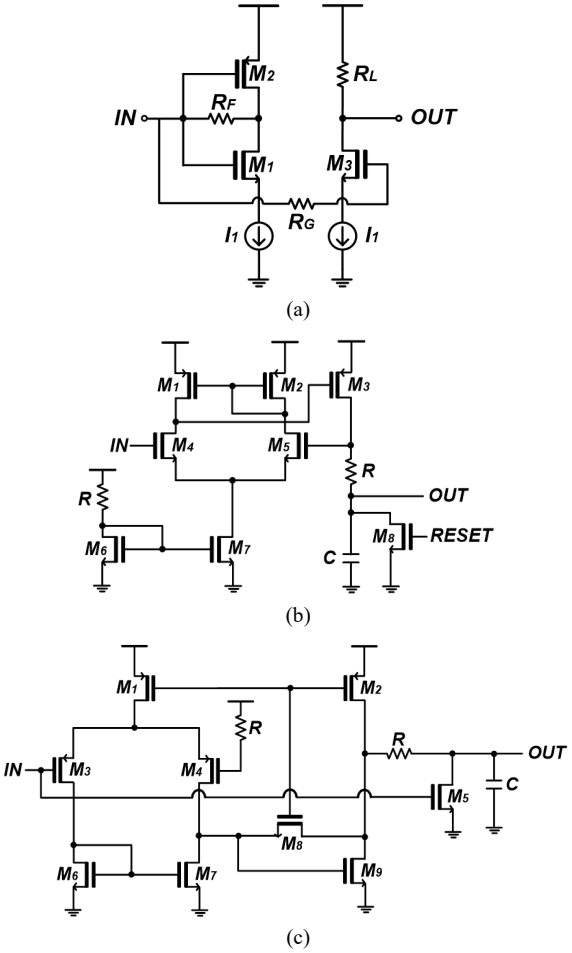

Fig. 4 Schematic diagrams of (a) VCF-TIA, (b) peak detect & hold circuit of A2V, and (c) Charging circuit of T2V.

Fig. 4(b) shows the schematic diagram of the peak detect & hold (PDH) circuit of A2V, where the PDH samples and holds the signals to guarantee limiting operations with an ideally infinite gain.

Fig. 4(c) depicts the schematic diagram of the charging circuit of T2V, which exploits an integrator with an MIM capacitor to generate a linear relationship of time-interval with the output voltage.

B. Chip Layout & Post-layout Simulation Results

Fig. 5 shows the layout of the proposed optoelectronic receiver IC, where the chip occupies the area of 2.1 x 2.0 mm^2, and consumes 262 mW in total from a 1.8-V supply.

Fig. 6 depicts the simulated transient responses of the A2V converter, enabling the recovery of input currents from 5 ~ 500 μA_{pp} with gain control scheme. This corresponds to the maximum detection range of 8.2 meters.

Fig. 7 shows the transient responses of the T2V converter, restoring the input currents of 50 μA_{pp} ~ 1.1 mA_{pp} that corresponds to the input dynamic range of 27 dB. This indicates a minimum detection range of 56 centimeters.

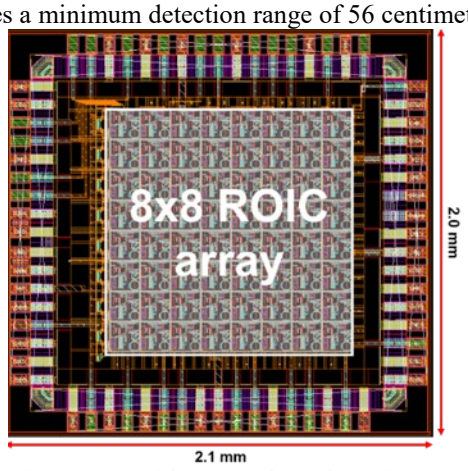

Fig. 5. Layout of the proposed optoelectronic ROIC.

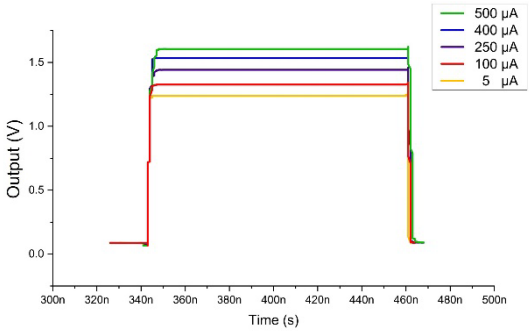

Fig. 6. Simulated pulse response of the proposed A2V with gain control scheme for different input currents.

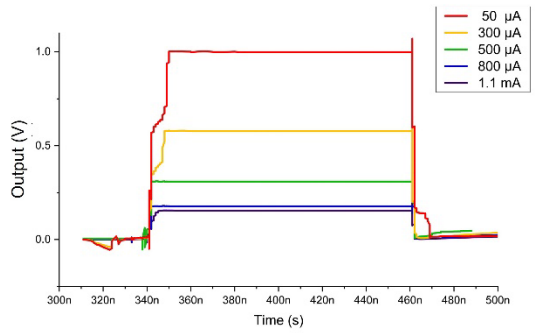

Fig. 7. Simulated pulse response of the proposed T2V.

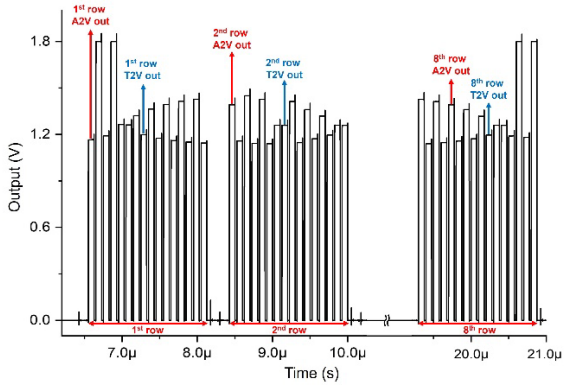

Fig. 8. Simulated final results of the 8x8 ROIC.

TABLE I. Performance Summary of the Proposed ROIC.

Parameters	[8]	This work
Supply voltage (V)	1.8	1.8
# of channels	16 x 1	8 x 8
Input current (mA_{pp})	0.001 ~ 1.1	0.005 ~ 1.1
A2V range (meter)	0.5 ~ 25	0.82 ~ 8.2
T2V range (meter)	N/A	0.56 ~ 2.6
Power dissipation per channel (mW)	29.8	4.1
Chip area (mm^2)	5 x 1.1	2 x 2.1

Fig. 8 illustrates the simulated final results of the whole 8x8 ROIC array, demonstrating the sequential output pulses from the 1st to the 8th row of A2V and T2V, respectively.

Table I compares the performance of the proposed optoelectronic ROIC with a previously reported 16 x 1 channel optical receiver array, where it is clearly seen that the proposed ROIC recovers both voltage amplitude and time interval with good linearity within a short detection range. Furthermore, it was designed with low power consumption and a small area, facilitating the implementation of multi-channel arrays for indoor-monitoring LiDAR applications.

Ⅲ. CONCLUSION

We have suggested an optoelectronic ROIC realized in a 180-nm CMOS technology for the applications of elder-care LiDAR sensors. It provides various advantages, such as lower cost, simpler integration, smaller package parasitics, etc. Conclusively, it is certain that this work enables to provide a potential for a low-cost sensor solution for short-range home-monitoring systems, especially to save single elders and/or dementia patients in cases of emergency.

ACKNOWLEDGMENT

The EDA tool was supported by the IC Design Education Center.

REFERENCES

[1] M. Montero-Odasso, J. Verghese, O. Beauchet, and J. M. Hausdorff, “Gait and Cognition: A Complementary Approach to Understanding Brain Function and the Risk of Falling,” J. of American Geriatrics Society, vol. 60, no. 11, pp. 2127–2136, Nov. 2012.

[2] B. D. Boer, J. Hamers, H. Beerens, S. Zwakhalen, F. Tan, and H. Verbeek, “Living at the farm, innovative nursing home care for people with dementia – study protocol of an observational longitudinal study,” BMC Geriatrics, vol. 15, no. 1, Feb. 2015.

[3] D. Yoon et al., “Mirrored Current-Conveyor Transimpedance Amplifier for Home Monitoring LiDAR Sensors,” IEEE Sensors J., vol. 21, pp. 5589-5597, 2021.

[4] T. H. Jin et al., “Time-of-Arrival Measurement Using Adaptive CMOS IR-UWB Range Finder with Scalable Resolution,” IEEE Tran. on Circuits and Systems-I, Vol. 63, No. 10, pp. 1605-1615, Oct. 2016.

[5] Y. Kim et al., “Novel Chest Compression Depth Measurement Sensor Using IR-UWB for Improving Quality of Cardiopulmonary Resuscitation,” IEEE Sensors J., Vol. 17, No. 10, pp. 3174-3183, May 2017.

[6] C. Hermans et al., “A high-speed 850-nm optical receiver front-end in 0.18-μm CMOS,” IEEE J. Solid-State Circuits, Vol. 41, No. 7, pp. 1606–1614, Jul. 2006.

[7] J. -E. Joo et al., “A CMOS Optoelectronic Receiver IC with an On-Chip Avalanche Photodiode for Home-Monitoring LiDAR Sensors,” Sensors, vol. 21, no. 13, pp. 4364, 2021.

[8] C. Hong et al., “A linear-mode LiDAR sensor using a multi-channel CMOS transimpedance amplifier array,” IEEE Sensors J., vol. 18, pp. 7032-7040, 2018.

[9] M. -J. Lee, W. -Y. Choi, “Effects of Parasitic Resistance on the Performance of Silicon APDs in Standard CMOS Technology,” IEEE Electron Device Letters, Vol. 37, No. 1, pp. 60~63, Jan. 2016.

Shinhae Choi received the B.S. degree in electronic and electrical engineering from Ewha Womans University, Korea, in 2023. Her current research interests include silicon photonics and CMOS optoelectronic integrated circuits and architectures for short-distance optical application systems and sensor interface IC designs.

Yeojin Chon received the B.S. degree in electronic and electrical engineering from Ewha Womans University, Korea, in 2022. Her current research interests include silicon photonics and CMOS optoelectronic integrated circuits and architectures for short-distance optical application systems and sensor interface IC designs.

Sung Min Park received the B.S. degree in electrical and electronic engineering from KAIST, Korea, in 1993. He received the M.S. degree in electrical engineering from University College London, U.K., in 1994, and the Ph.D. degree in electrical and electronic engineering from Imperial College London, U.K., in May 2000. In 2004, he joined the faculty of the Department of Electronics Engineering at Ewha Womans University in Seoul, Korea, where he is currently a professor.